Valence fluctuations in ferromagnetic 4f systems

W. Nolting and A. Ramakanth*
Institut für Theoretische Physik II, Domagkstrasse 75, 4400 Münster, Federal Republic of Germany
(Received 5 August 1985)

We investigate the coexistence of ferromagnetism and intermediate valence in $4f$ systems which have ferromagnetic ground states in the normal-valence phase and fluctuate between a magnetic ($J\neq 0$) and a nonmagnetic ($J=0$) state in the intermediate-valence phase. We use a model which is generated from the well-known s-f model by inclusion of a hybridization term. The alloy analogy of the model is solved for zero temperature in the average T-matrix approximation. For the local magnetic $4f$ moment m_f we derive phase diagrams in terms of the hybridization V, the bandwidth W (closely related to external pressure), the direct exchange J_0, and the s-f exchange g ($g>0$). The hybridization V, as well as a gap reduction as a consequence of a pressure-induced band broadening, intensify electronic fluctuations and therefore tend to destabilize the local moment, while the exchange integrals g and J_0 favor the opposite. We find regions of saturated ($m_f=n_f$), reduced ($0<m_f<n_f$), and quenched f moments ($m_f=0$) even in intermediate-valence phases. Quasiparticle densities of states for typical parameter constellations are derived and discussed. They show an ever-existing hybridization gap.

I. INTRODUCTION

Intermediate valence phases of certain $4f$ systems stand out for some extraordinary physical properties.[1] Observed exclusively in Ce, Pr, Sm, Eu, Tm and Yb compounds the phenomenon of intermediate valence is due to the fact that the respective rare-earth ions can in principle exist in two different valence states with different numbers of $4f$ electrons. Temperature and pressure variations, or alloying with proper impurities, may lead to a quasidegeneration of the two valence states, giving rise to a nonintegral average occupation number of the $4f$ shell. The transition from the normal into the intermediate-valence phase is accompanied by striking changes in the physical properties,[1] which justify the high interest these $4f$ systems have gained in the recent past.

In our opinior the magnetic anomalies of the intermediate-valence phases evoke a special fascination. It is a momentous fact that with the exceptions of Tm and Pr, all $4f$ systems with valence instabilities fluctuate between a magnetic ($J\neq 0$) and a nonmagnetic ($J=0$) configuration, which must lead to some destabilization of the local f moment. The question whether there is a partial or even a total quenching of the local moment becomes particularly important in materials which show a collective (ferro- or antiferromagnetic) ordering of the moments in their normal valence ground states, e.g., EuO, CePt, $CeRh_3B_2$, $EuAu_2Si_2$. How strong must be the electronic fluctuations in order to destroy the collective magnetism? Is there any coexistence of intermediate valence and magnetic order? The present paper aims at a certain clarification of these fundamental questions. Right at the outset we would like to point out that we exclusively discuss here $4f$ systems which fluctuate between a magnetic ($J\neq 0$) and a nonmagnetic ($J=0$) configuration, e.g., Eu and Ce compounds. The antiferromagnetic ordering of mixed valence TmSe, which fluctuates between two magnetic configurations may be understood by Varma's double-exchange model.[2]

There are a lot of experimental data which seem to indicate that under certain circumstances a coexistence of magnetism and intermediate valence may be possible, particularly in Eu- and Ce-based $4f$ systems. High-pressure experiments on the classical Heisenberg ferromagnet EuO (Ref. 3) show two first-order phase transitions, a structural one ($NaCl\rightarrow CsCl$) at about 400 kbar, and an isostructural insulator metal transition at about 300 kbar accompanied by a substantial volume decrease of nearly 5%. The experiments have been performed at room temperature, so that EuO is thought to be paramagnetic. One of us[4] has explained this pressure-induced electronic transition within the framework of an "extended" s-f model, similar to the model we use in this paper. The basic assumption of the theory was that EuO is indeed paramagnetic at $T=300$ K. Very recently, however, the just-mentioned pressure experiment has been repeated by Zimmer *et al.*[5] resulting in a striking discrepancy to the previous one.[3] These authors found that the insulator-metal transition sets in already at a very much lower pressure of about 140 kbar, and extends over a huge pressure interval. A satisfying explanation of the latter experiment needs the assumption that under high pressure EuO is ferromagnetic at room temperature. If it is so, then the well-known red shift of the lower conduction-band edge, typical for ferromagnetic semiconductors like EuO,[6] brings about an additional gap reduction. This would explain the relatively low critical pressure. Further, the smooth transition extending over a large pressure interval can be understood by the following reasoning. As a consequence of an s-f (or better d-f) exchange interaction the edge shift is bound to the existence of localized magnetic $4f$ moments. If, however, one of the $4f$ electrons tunnels into the conduction band, then the nonmagnetic $(4f)^6$ configuration of Eu^{3+} is left behind. This leads at least to a dilution of the

localized moment system, possibly even to an additional moment quenching. That means, however, that the gap will increase since the exchange-caused edge shift will be reduced. Electrons then flood back into the localized $4f$ levels, the moment system becomes more perfect again, so that the edge shift increases again, and so on. Therefore a dynamic interplay between the dilution of the moment system and the sensitive reaction of the conduction-band density of states is to be expected, which may result in a smooth transition extending, as observed, over a huge pressure interval. But is ferromagnetic ordering in EuO at room temperature a realistic assumption when normal-valent EuO has $T_c = 69.33$ K? Contrary to the common opinion that s-f (or d-f) hybridization destroys ferromagnetism, one would have to assume that it leads rather to an *enhancement* of the ferromagnetic coupling just in the intermediate-valence phase. To clarify the situation we need a self-consistent determination of the pressure dependence of the average f-level occupation (valence), the local $4f$ moment and the Curie temperature T_c. This is the aim of our investigations.

There exists, indeed, some experimental support that a gap reduction may lead to a drastic enhancement of the ferromagnetic coupling in such $4f$ systems. Gignoux and Voiron[7] have measured the Curie temperature of $CeNi_xPt_{1-x}$ as function of the Ni content x. CePt is a normal valent ferromagnetic $4f$ system with $T_c \approx 6$ K. On the other side, CeNi is an intermediate-valent Pauli paramagnet. Roughly speaking, alloying CePt with Ni means reducing the distance between $4f$ level and Fermi edge. With increasing x the local Ce moment decreases, but nevertheless T_c shows first a dramatic increase reaching a distinct maximum and then breaks down very abruptly in the intermediate-valence phase. Similar tendencies are observed in antiferromagnetic $Eu(Pd_{1-x}Au_x)_2Si_2$.[8] Malik *et al.*[9] explain the high Curie temperature ($T_c \approx 115$ K) of $CeRh_3B_2$ by a strong hybridization of localized Ce-$4f$ electrons with conduction electrons. All these experimental data find a qualitatively satisfying interpretation by the theory of Matlak and Nolting,[10,11] based on a "mean-field" version of an "extended" s-f model, which will be the starting point for the present paper, too (Sec. II).

The main purpose of our investigations is to find out what happens to the ferromagnetic order in $4f$ systems such as EuO when forced by pressure, e.g., into an intermediate-valence phase. Special attention is devoted to the competitive influence of the s-f exchange and s-f hybridization on the stability of the local $4f$ moment. The results will be presented as phase diagrams constructed in dependence of relevant model parameters. Typical for $4f$ systems like EuO is a *positive* s-f exchange. The Anderson model, frequently used for describing the intermediate-valence phenomenon, is therefore an inappropriate starting point for these systems because the Shrieffer-Wolff transformation of this model leads to an *antiferromagnetic* s-f exchange. It is, however, well known that normal valent magnetic $4f$ systems as the Eu chalcogenides are excellently described by the s-f model.[6] Thus it suggests itself to start with this model, which, however, must be extended by a hybridization term which allows electronic transitions between $4f$ level and conduction band. This "extended" s-f model is introduced in Sec. II. Section III presents an alloy analogy of this model, which is solved in Sec. IV by a T-matrix procedure. Results for the quasiparticle densities of states lead to some phase diagrams revealing the stability of the local f moment. This is discussed in Sec. V.

II. "HYBRIDIZED" s-f MODEL

We use a model which properly takes into account interactions and correlations between itinerant conduction electrons and localized $4f$ electrons on a rare-earth compound with a ferromagnetic ground state in its normal valence phase:

$$H = H_s + H_f + H_{sf} + H_v \ . \tag{2.1}$$

The conduction electrons are considered as s electrons with an intraatomic Coulomb interaction U_c

$$H_s = \sum_{i,j,\sigma} T_{ij} c_{i\sigma}^{\dagger} c_{j\sigma} + \tfrac{1}{2} U_c \sum_{i,\sigma} n_{i\sigma}^{(c)} n_{i,-\sigma}^{(c)} \ , \tag{2.2}$$

$c_{i\sigma}$ and $c_{i\sigma}^{\dagger}$ are, respectively, annihilation and creation operator of an s electron with spin σ at site $\mathbf{R}_i$. $n_{i\sigma}^{(c)} = c_{i\sigma}^{\dagger} c_{i\sigma}$ is the number operator. T_{ij} are the usual hopping integrals being related to the Bloch energies $\epsilon(\mathbf{k})$ by

$$T_{ij} = \frac{1}{N} \sum_{\mathbf{k}} \epsilon(\mathbf{k}) e^{i\mathbf{k}\cdot(\mathbf{R}_i - \mathbf{R}_j)} \ . \tag{2.3}$$

We assume a nondegenerate f-level $E_{f\sigma}$, and a very large Coulomb-interaction U_f, in order to guarantee that the level is at most singly occupied

$$H_f = \sum_{i,\sigma} E_{f\sigma} f_{i\sigma}^{\dagger} f_{i\sigma} + \tfrac{1}{2} U_f \sum_{i,\sigma} n_{i\sigma}^{(f)} n_{i,-\sigma}^{(f)} \ . \tag{2.4}$$

The empty f level is attributed to the nonmagnetic configuration $J = 0$ [$(4f)^6$ in the case of EuO], the singly occupied level to the magnetic configuration $J \neq 0$ [$(4f)^7$ in the case of EuO]. $f_{i\sigma}^{\dagger}$ and $f_{i\sigma}$ are the construction operators for f electrons with spin σ; $n_{i\sigma}^{f} = f_{i\sigma}^{\dagger} f_{i\sigma}$ is the number operator.

Because of the normally negligible overlap of $4f$ wave functions, centered at different sites, the direct exchange of the localized magnetic $4f$ moments should contribute only very little. We use the direct exchange, if at all, only in its simplified mean-field version,

$$E_{f\sigma} = E_f - z_\sigma J_0 m_f \quad (z_\uparrow = +1, z_\downarrow = -1) \ . \tag{2.5}$$

If we choose the exchange constant $J_0 \neq 0$, then we have to calculate the "magnetization" m_f of the f level

$$m_f = \sum_{\sigma} z_\sigma \langle n_{i\sigma}^{(f)} \rangle \ , \tag{2.6}$$

self-consistently, of course, within our model.

The most important part of the Hamiltonian (2.1) is the intra-atomic s-f exchange interaction H_{sf} between localized $4f$ moments and conduction electrons. This coupling does exist, however, only if the respective lattice site is actually found in its magnetic $4f$ configuration ($J = S = \frac{7}{2}$

for EuO). This fact is taken into account by a statistical variable p_i,

$$p_i=\begin{cases}0 & \text{if } J=0 \text{ at site } \mathbf{R}_i\\ 1 & \text{if } J\neq 0 \text{ at site } \mathbf{R}_i,\end{cases} \tag{2.7}$$

being inserted into the s-f interaction[6]

$$H_{sf}=-\tfrac{1}{2}g\sum_{i,\sigma}p_i(z_\sigma S_i^z n_{i\sigma}^{(c)}+S_i^\sigma c_{i,-\sigma}^\dagger c_{i\sigma}) , \tag{2.8}$$

g is the s-f coupling constant, and $\mathbf{S}_i=(S_i^x,S_i^y,S_i^z)$ is the localized $4f$ spin with

$$S_j^\sigma=S_j^x+iz_\sigma S_j^y . \tag{2.9}$$

This spin operator must be connected with the f operators $f_{i\sigma}$, $f_{i\sigma}^\dagger$, and $n_{i\sigma}^{(f)}$ in a self-consistent manner, which indeed becomes possible by the alloy analogy to be developed in the Sec. III for the "hybridized" s-f model (2.1). As shown in detail in Ref. 12 for normal valent $4f$ systems ($p_i\equiv 1$), the s-f interaction H_{sf} causes dramatic shifts and splittings of the Bloch band with striking temperature and carrier concentration-dependent densities of states. Similar effects should appear in the intermediate-valence phase, too, at least as long as there are localized magnetic moments. We are therefore convinced that H_{sf} plays a dominant role that concerns the problem under study.

Finally the original s-f model has to be extended by a hybridization term H_v,

$$H_v=V\sum_{i,\sigma}(c_{i\sigma}^\dagger f_{i\sigma}+f_{i\sigma}^\dagger c_{i\sigma}) , \tag{2.10}$$

which enables electronic transitions between the $4f$ level and the conduction band. Since the total electron number cannot change, we can use the condition

$$n_c+n_f=n_0=\text{const} , \tag{2.11}$$

$$n_{c,f}=\sum_\sigma\langle n_{i\sigma}^{(c,f)}\rangle , \tag{2.12}$$

in order to fix the chemical potential μ.

The model contains some parameters. In order to be concrete, we have chosen values which should be realistic for EuO,[6,12] e.g., $g=0.2$ eV, $U_f=100$ eV, $S=\frac{7}{2}$, $n_0=1$. An important model parameter is the Bloch density of states ρ_0, for which we use throughout the paper the following simple triangular shape:[12]

$$\rho_0(E)=\begin{cases}\dfrac{2}{W^2}(E+\frac{2}{3}W) & \text{if } -\frac{2}{3}W\leqq E\leqq\frac{1}{3}W\\ 0 & \text{otherwise} .\end{cases} \tag{2.13}$$

The center of gravity of the Bloch band defines the energy zero ($T_{ii}=T_0=0$). Normal EuO has a Bloch bandwidth $W\approx 2$ eV and a gap E_g between f level and conduction band of 1.12 eV. As explained in detail in Ref. 4 the s-f interaction takes care for a paramagnetic edge shift of 0.09 eV relative to the Bloch band edge at $-\frac{2}{3}W=-1.33$ eV. So the f level of normal valent EuO is at $E_f=-2.54$ eV.

Usually the pressure dependence of the gap is taken into account by a respective shift of the f-level E_f towards the lower edge of the conduction band, while the bandwidth is fixed at a constant value. In our opinion, however, applying pressure means, strictly speaking, a broadening of the conduction band, while E_f as an intraatomic property should not change very much. This is a very important point. In Ref. 13 it is shown that the physics of the s-f model is strikingly dependent on the ratio W/g. So, if we are sure that the closing of the gap is indeed due to a broadening of the band, then we should take this fact explicitly into account. The change in W by itself leads to drastic modifications in the physical properties of the system. We have therefore fixed the distance between $4f$ level and the center of gravity of the Bloch band at a constant value, simulating the pressure dependence of the gap by a pressure-dependent Bloch bandwidth $W(p)$.

It is, however, clear that the "extended" s-f model, defined by the Hamiltonian (2.1), is not exactly solvable. Approximations must be tolerated. For this purpose we develop in the Sec. III an alloy analogy of this model. One of us has used such an alloy analogy in the case of the "normal" s-f model in connection with an average T-matrix approximation[12] (ATA) and a coherent-potential approximation[14,15] (CPA), respectively. The results are quite convincing, as can be seen by comparison with exactly solvable limiting cases as well as with other approximate theories. So we believe the alloy analogy to be a reliable procedure for the extended s-f model, too. Further support may be deduced from similar treatments of the intermediate-valence phenomenon within the framework of closely related models such as the Anderson model[16,17] and the Falicov-Kimball model.[18,19]

III. ALLOY ANALOGY

The appearance of the statistical variable p_i (2.7) in the model Hamiltonian (2.1) strongly suggests an alloy analogy for solving the many-body problem in the following sense. If a $\uparrow$ electron propagates through the lattice it will meet three different kinds of lattice sites. It can come across the magnetic $4f$ configuration, realized in our model by the presence of a $\uparrow$- or a $\downarrow$-f electron, respectively, or the nonmagnetic configuration, realized by an empty f level.

If an s electron with spin σ finds a magnetic place ($p_i=1$), then the normal intraatomic s-f interaction sets in. The full analytical solution of the zero bandwidth s-f model given in Ref. 20 tells us that the s-f interaction splits the s level T_0 into three quasiparticle levels,

$$\begin{aligned}\epsilon_1&=T_0-\tfrac{1}{2}gS ,\\ \epsilon_2&=T_0+\tfrac{1}{2}g(S+1) ,\\ \epsilon_3&=T_0+U_c+\tfrac{1}{2}gS ,\end{aligned} \tag{3.1}$$

with strongly spin-, temperature-, and carrier concentration dependent spectral weights:

$$\alpha_{1\sigma}=\frac{2S+2-n_c}{2(2S+1)}+z_\sigma\langle S^z\rangle\frac{2S+2-n_c}{2(2S+1)(S+1-n_c)} , \tag{3.2}$$

$$\alpha_{2\sigma}=\frac{S(1-n_c)}{2S+1}-z_\sigma\langle S^z\rangle\frac{(S+1)(1-n_c)}{(2S+1)(S+1-n_c)}\ , \tag{3.3}$$

$$\alpha_{3\sigma}=\frac{n_c}{2}-z_\sigma\langle S^z\rangle\frac{n_c}{2(S+1-n_c)}\ . \tag{3.4}$$

According to Ref. 14, (3.1)–(3.4) are valid for $n_c\leqq 1$, as in our case here, because we have $n_0=1$ in (2.11).

If the s electron enters a nonmagnetic site ($p_i=0$) s-f interaction becomes of course impossible. Two energy levels are available, depending on whether there is another s electron with opposite spin or not

$$\epsilon_5=T_0;\quad \epsilon_6=T_0+U_c\ . \tag{3.5}$$

The corresponding weights are

$$\alpha_{5\sigma}=1-\alpha_{3\sigma};\quad \alpha_{6\sigma}=\alpha_{3\sigma}\ . \tag{3.6}$$

Similar considerations for an f electron lead, according to (2.4), to two different atomic levels $E_{f\sigma}$ and $E_{f\sigma}+U_f$ with spectral weights $(1-n_{f-\sigma})$ and $n_{f-\sigma}$, respectively.

For our coupled electron system we have to combine all these possibilities, so that there are in the real crystal eight different situations for a propagating electron, which are listed in Table I.

We now replace the real system by a fictitious alloy consisting of eight two-level components according to the eight atomic levels $\eta_{i\sigma}^{(s,f)}$. The constituents of this alloy are randomly distributed over the lattice with certain concentrations, which we identify with the spectral weights $\gamma_{i\sigma}$ of the atomic levels $\eta_{i\sigma}^{(s,f)}$ (Table I). For a propagating electron it should then mean quite the same situation, either to move in the real crystal or to move in this fictitious alloy.

The "concentrations" $\gamma_{i\sigma}$ depend in a rather complicated manner on quantities such as the average occupation numbers n_c and n_f, which have to be determined self-consistently within our model. Furthermore, the $\gamma_{i\sigma}$ depend also on the $4f$ magnetization $\langle S^z\rangle$ coming into play via the weights $\alpha_{i\sigma}$ of the normal atomic s-f model [(3.2)–(3.4)]. This expectation value must be connected with the magnetization m_f of the nondegenerate f level. The ansatz

$$\langle S^z\rangle\approx S\frac{m_f}{n_f} \tag{3.7}$$

is exact for $S=\frac{1}{2}$ and should be a reasonable approximation for $S>\frac{1}{2}$, too. If we accept Eq. (3.7) and use

$$n_{f\sigma}=\tfrac{1}{2}(n_f+z_\sigma m_f)\ , \tag{3.8}$$

then the "concentrations" $\gamma_{i,-\sigma}$ are completely determined by n_c, n_f, and m_f, where n_c and n_f are in addition connected by the self-consistency condition (2.11).

TABLE I. The spectral weights $\gamma_{i\sigma}$ of the atomic levels $\eta_{i\sigma}^{(s,f)}$.

Spectral weights	s levels	f levels
$\gamma_{1\sigma}=n_{f-\sigma}\alpha_{1\sigma}$	$\eta_{1\sigma}^{(s)}=\epsilon_1$	$\eta_{1\sigma}^{(f)}=E_{f\sigma}+U_f$
$\gamma_{2\sigma}=n_{f-\sigma}\alpha_{2\sigma}$	$\eta_{2\sigma}^{(s)}=\epsilon_2$	$\eta_{2\sigma}^{(f)}=E_{f\sigma}+U_f$
$\gamma_{3\sigma}=n_{f-\sigma}\alpha_{3\sigma}$	$\eta_{3\sigma}^{(s)}=\epsilon_3$	$\eta_{3\sigma}^{(f)}=E_{f\sigma}+U_f$
$\gamma_{4\sigma}=n_{f\sigma}\alpha_{1\sigma}$	$\eta_{4\sigma}^{(s)}=\epsilon_1$	$\eta_{4\sigma}^{(f)}=E_{f\sigma}$
$\gamma_{5\sigma}=n_{f\sigma}\alpha_{2\sigma}$	$\eta_{5\sigma}^{(s)}=\epsilon_2$	$\eta_{5\sigma}^{(f)}=E_{f\sigma}$
$\gamma_{6\sigma}=n_{f\sigma}\alpha_{3\sigma}$	$\eta_{6\sigma}^{(s)}=\epsilon_3$	$\eta_{6\sigma}^{(f)}=E_{f\sigma}$
$\gamma_{7\sigma}=(1-n_f)(1-\alpha_{3\sigma})$	$\eta_{7\sigma}^{(s)}=\epsilon_5$	$\eta_{7\sigma}^{(f)}=E_{f\sigma}$
$\gamma_{8\sigma}=(1-n_f)(1-\alpha_{3\sigma})$	$\eta_{8\sigma}^{(s)}=\epsilon_6$	$\eta_{8\sigma}^{(f)}=E_{f\sigma}$

In the just-developed alloy picture the model Hamiltonian (2.1) is replaced by the following expression:

$$\overline{H}=\sum_{ij\sigma}^{i\neq j}T_{ij}c_{i\sigma}^\dagger c_{j\sigma}+V\sum_{i,\sigma}(f_{i\sigma}^\dagger c_{i\sigma}+c_{i\sigma}^\dagger f_{i\sigma})+\sum_{i,\sigma}(\eta_{s\sigma}^{(i)}c_{i\sigma}^\dagger c_{i\sigma}+\eta_{f\sigma}^{(i)}f_{i\sigma}^\dagger f_{i\sigma})\ . \tag{3.9}$$

The third term contains random variables $\eta_{s(f)\sigma}^{(i)}$ which can be one of the eight values listed in Table I:

$$\eta_{s\sigma}^{(i)}\in\{\eta_{1\sigma}^{(s)},\ldots,\eta_{8\sigma}^{(s)}\}\ ,\qquad \eta_{f\sigma}^{(i)}\in\{\eta_{1\sigma}^{(f)},\ldots,\eta_{8\sigma}^{(f)}\}\ . \tag{3.10}$$

The lack of translational symmetry, due to these random variables, is removed by the usual configuration averaging, which leads to an effective Hamiltonian $H_{\rm eff}$,

$$\mathbf{H}\rightarrow H_{\rm eff}=\sum_{ij\sigma}[T_{ij}+M_{ij\sigma}^{(s)}(E)]c_{i\sigma}^\dagger c_{j\sigma}+\sum_{ij\sigma}M_{ij\sigma}^{(f)}(E)f_{i\sigma}^\dagger f_{j\sigma}+\sum_{i,\sigma}\tilde{V}_\sigma(E)(c_{i\sigma}^\dagger f_{i\sigma}+f_{i\sigma}^\dagger c_{i\sigma})\ . \tag{3.11}$$

$H_{\rm eff}$ possesses the full symmetry of the lattice, but is now non-Hermitian and energy dependent. The latter complications are introduced by the self-energies $M_{ij\sigma}^{(s)}$ and $M_{ij\sigma}^{(f)}$ of the s and f electrons, and by a renormalization of the hybridization matrix element $\tilde{V}_\sigma(E)$. $M_{ij\sigma}^{(s)}$, $M_{ij\sigma}^{(f)}$, and $\tilde{V}_\sigma$ contain all interaction processes taking place in the underlying electron system. After having determined these terms, explicitly done in Sec. IV, the further procedure is straightforward. All the information we are interested in can be deduced from the configuration-averaged one-electron Green function $G_{\mathbf{k}\sigma}(E)$, which is here a 2×2 matrix being easily derived from (3.11),

$$G_{\mathbf{k}\sigma}(E)=\langle\mathbf{k}_\sigma|[E-H_{\rm eff}(E)]^{-1}|\mathbf{k}\sigma\rangle=\begin{bmatrix}G_{\mathbf{k}\sigma}^{(s)}(E) & G_{\mathbf{k}\sigma}^{(sf)}(E)\\ G_{\mathbf{k}\sigma}^{(fs)}(E) & G_{\mathbf{k}\sigma}^{(f)}(E)\end{bmatrix}=D_{\mathbf{k}\sigma}^{-1}(E)\begin{bmatrix}E-M_{\mathbf{k}\sigma}^{(f)}(E) & \tilde{V}_\sigma(E)\\ \tilde{V}_\sigma(E) & E-\epsilon(\mathbf{k})-M_{\mathbf{k}\sigma}^{(s)}(E)\end{bmatrix}. \tag{3.12}$$

$M_{\mathbf{k}\sigma}^{(s,f)}$ are the $\mathbf{k}$-dependent Fourier transforms of $M_{ij\sigma}^{(s,f)}$, and $D_{\mathbf{k}\sigma}(E)$ is a short-hand notation for

$$D_{\mathbf{k}\sigma}(E)=[E-\epsilon(\mathbf{k})-M_{\mathbf{k}\sigma}^{(s)}(E)][E-M_{\mathbf{k}\sigma}^{(f)}(E)]-\tilde{V}_\sigma^2(E)\ . \tag{3.13}$$

The imaginary parts of the respective s and f Green func-

tions determine the s- and f-quasiparticle densities of states $\rho_\sigma^{(s,f)}(E)$,

$$\rho_\sigma^{(s,f)}(E)=-\frac{1}{N\pi}\sum_{\mathbf{k}}\mathrm{Im}G_{\mathbf{k}\sigma}^{(s,f)}(E)\ . \tag{3.14}$$

From these densities of states we get the average occupation numbers $n_{c,f\sigma}$,

$$n_{c,f\sigma}=\int_{-\infty}^{+\infty}dE\,\rho_\sigma^{(s,f)}(E)\{1+\exp[\beta(E-\mu)]\}^{-1} \qquad \left[\beta=\frac{1}{k_BT}\right], \tag{3.15}$$

which we need to fix self-consistently the spectral weights $\gamma_{i\sigma}$ of our fictitious alloy. Furthermore, via $m_{f,c}=\sum_\sigma z_\sigma n_{f,c\sigma}$ they answer the question under what demands on model parameters such as V, W, J_0, and g collective magnetism occurs.

IV. T-MATRIX AND SELF-ENERGY

The remaining task is the determination of the self-energies $M_{\mathbf{k}\sigma}^{(s,f)}(E)$ and the renormalized hybridization $\tilde{V}_\sigma(E)$. We use a T-matrix procedure[15] similar to that of Ref. 12. First we decompose the Hamiltonian $\overline{H}$ (3.9) in an exactly tractable part K_σ and another part Q_σ, which contains the random variables

$$\overline{H}=\sum_\sigma\overline{H}_\sigma=\sum_\sigma(K_\sigma+Q_\sigma)\ , \tag{4.1}$$

$$K_\sigma=\sum_{i,j}(T_{ij}+B_{s\sigma}\delta_{ij})c_{i\sigma}^\dagger c_{j\sigma}+\sum_i B_{f\sigma}f_{i\sigma}^\dagger f_{i\sigma} +V\sum_i(c_{i\sigma}^\dagger f_{i\sigma}+f_{i\sigma}^\dagger c_{i\sigma})\ , \tag{4.2}$$

$$Q_\sigma=\sum_i(v_{s\sigma}^{(i)}c_{i\sigma}^\dagger c_{i\sigma}+v_{f\sigma}^{(i)}f_{i\sigma}^\dagger f_{i\sigma})\ , \tag{4.3}$$

$$v_{s,f\sigma}^{(i)}=\eta_{s,f\sigma}^{(i)}-B_{s,f\sigma}\ . \tag{4.4}$$

Here we have introduced "effective media" $B_{s,f\sigma}$ for s and f electrons, respectively, which can be chosen so that K_σ is already a good first-order approximation of the full Hamiltonian. On the other hand, the problem arising with K_σ has to remain exactly solvable.

For the s electrons, which move in a relatively broad conduction band, a so-called "virtual crystal approximation"[15] should be a reasonable ansatz,

$$B_{s\sigma}=\sum_{i=1}^{8}\gamma_{i\sigma}\eta_{i\sigma}^{(s)}\ , \tag{4.5}$$

while for the relatively sharp f level an "atomic limit" ansatz is more obvious. We therefore determine $B_{f\sigma}$ from

$$\frac{1}{E-B_{f\sigma}}=\frac{1-n_{f-\sigma}}{E-E_{f\sigma}}+\frac{n_{f-\sigma}}{E-E_{f\sigma}-U_f}\ . \tag{4.6}$$

$B_{f\sigma}$ is then energy dependent,

$$B_{f\sigma}=\frac{E_{f\sigma}(E-E_{f\sigma}-U_f)+En_{f-\sigma}U_f}{(E-E_f-U_f)+n_{f-\sigma}U_f}\ . \tag{4.7}$$

Since K_σ is thought to be already configuration averaged, the Hamiltonian H_{eff} (3.11) can always be written in the following form:

$$H_{\mathrm{eff}}=\sum_\sigma H_{\mathrm{eff},\sigma}=\sum_\sigma(K_\sigma+\Sigma_\sigma)\ . \tag{4.8}$$

We denote by $R_\sigma(E)$ the one-electron Green function of the effective medium

$$R_\sigma(E)=\frac{1}{E-K_\sigma} \tag{4.9}$$

and by $G_\sigma(E)$ that of the "full" system,

$$G_\sigma(E)=\frac{1}{E-\overline{H}_\sigma}=\frac{1}{E-K_\sigma-Q_\sigma}\ . \tag{4.10}$$

Configuration averaging does not affect $R_\sigma(E)$, but it does affect $G_\sigma(E)$,

$$\langle G_\sigma(E)\rangle=\frac{1}{E-H_{\mathrm{eff},\sigma}(E)}=\frac{1}{E-K_\sigma(E)-\Sigma_\sigma(E)}\ . \tag{4.11}$$

From (4.9) to (4.11) we get the Dyson equations,

$$G_\sigma=R_\sigma+R_\sigma Q_\sigma G_\sigma\ , \tag{4.12}$$

$$\langle G_\sigma\rangle=R_\sigma+R_\sigma\Sigma_\sigma\langle G_\sigma\rangle\ , \tag{4.13}$$

which can be connected with the corresponding T-matrix equations:

$$G_\sigma=R_\sigma+R_\sigma T_\sigma R_\sigma\ , \tag{4.14}$$

$$\langle G_\sigma\rangle=R_\sigma+R_\sigma\langle T_\sigma\rangle R_\sigma\ . \tag{4.15}$$

A combination of the latter four equations then yields

$$\Sigma_\sigma=(\langle T_\sigma\rangle^{-1}+R_\sigma)^{-1}\ , \tag{4.16}$$

$$T_\sigma=(Q_\sigma^{-1}-R_\sigma)^{-1}\ . \tag{4.17}$$

If we switch off all atomic scatterers except one, then the full T matrix T_σ passes into the atomic scattering matrix $t_\sigma^{(i)}$,

$$t_\sigma^{(i)}=[(v_\sigma^{(i)})^{-1}-R_\sigma]^{-1}\ , \tag{4.18}$$

where $v_\sigma^{(i)}$ is a 2×2 matrix

$$v_\sigma^{(i)}=\begin{bmatrix}\eta_{s\sigma}^{(i)}-B_{s\sigma} & 0\\ 0 & n_{f\sigma}^{(i)}-B_{f\sigma}\end{bmatrix}, \tag{4.19}$$

built up according to (4.4) by random variables. The configuration averaging of the atomic T matrix reads as

$$\langle t_\sigma\rangle=\sum_{m=1}^{8}\gamma_{m\sigma}t_\sigma^{(m)}\ . \tag{4.20}$$

In order to determine the self-energy Σ_σ by Eq. (4.16) we need the full configuration-averaged T matrix $\langle T_\sigma\rangle$. This cannot be done rigorously. We apply the well-known "average T-matrix approximation[15] (ATA)," which is performed in detail in Ref. 12, where it has been shown to give quite reasonable results for the "normal" s-f model. Furthermore, it has been shown by Schwartz *et al.*[21] that the ATA yields results of comparable quality as the commonly accepted CPA. On the other hand, ATA is mathematically much easier to treat than CPA. Within ATA the T matrix $\langle T_\sigma\rangle$ reads as[12]

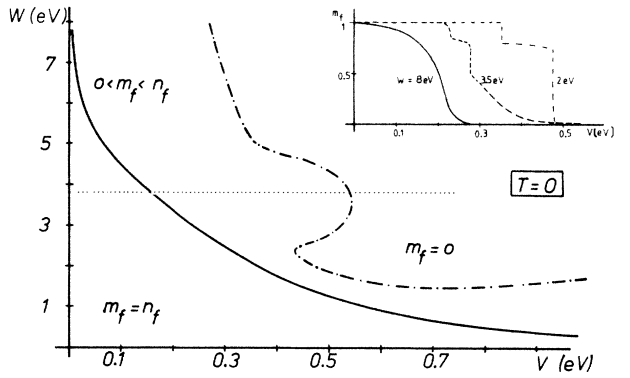

FIG. 1. Phase diagram for the local magnetic f moment m_f in terms of s-f hybridization V and Bloch bandwidth W. The solid line separates the regions of saturated ($m_f=n_f$) and reduced ($0<m_f<n_f$) f moment. To the right of the dashed-dotted phase line m_f is zero. The inset shows the f moment as a function of V for three different bandwidths. Parameters: $T=0$, $S=7/2$, $g=0.2$ eV, $J_0=0.005$ eV, $E_f=-2.54$ eV, $U_c=2$ eV, $U_f=100$ eV.

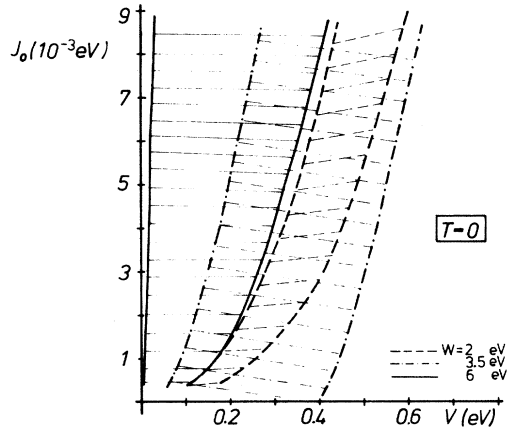

FIG. 2. Phase diagram for the local magnetic f moment m_f in terms of s-f hybridization and direct exchange J_0 for three different values of the Bloch bandwidth W (——, $W=6$ eV; —·—·—·, $W=3.5$ eV; — — —, $W=2$ eV). Other parameters as in Fig. 1. As a guide to the eye the reduced moment regions ($0<m_f<n_f$) are hatched. To the left of these regions the moment is saturated, to the right totally quenched.

$$\langle T_\sigma\rangle^{\mathrm{ATA}}=(\langle t_\sigma\rangle^{-1}-R_\sigma+R_{ii\sigma}\cdot\mathbf{1})^{-1} \tag{4.21}$$

so that with (4.16) the self-energy Σ_σ can be expressed by the atomic T matrix $\langle t_\sigma\rangle$, only

$$\Sigma_\sigma^{\mathrm{ATA}}=(\langle t_\sigma\rangle^{-1}+R_{ii\sigma}\cdot\mathbf{1})^{-1}\ . \tag{4.22}$$

$R_{ii\sigma}(E)$ is the diagonal element of $R_\sigma(E)$ in the spatial representation,

$$R_{ij\sigma}(E)=\langle i\sigma\,|\,R_\sigma(E)\,|\,j_\sigma\rangle\ . \tag{4.23}$$

As a special consequence of our approximation the self-energy is diagonal in the Wannier representation, and therefore $\mathbf{k}$ independent in the Bloch representation.

If we define

$$\Sigma_\sigma(E)=(\langle t_\sigma\rangle^{-1}+R_{ii\sigma}\cdot\mathbf{1})^{-1}=\begin{pmatrix}\Sigma_{s\sigma}(E) & \Sigma_{sf\sigma}(E)\\ \Sigma_{fs\sigma}(E) & \Sigma_{f\sigma}(E)\end{pmatrix} \tag{4.24}$$

and, furthermore,

$$M_{\mathbf{k}\sigma}^{(s)}(E)=M_\sigma^{(s)}=B_{s\sigma}+\Sigma_{s\sigma}(E)\ , \tag{4.25}$$

$$M_{\mathbf{k}\sigma}^{(f)}(E)=M_\sigma^{(f)}=B_{f\sigma}(E)+\Sigma_{f\sigma}(E)\ , \tag{4.26}$$

$$\tilde{V}_\sigma(E)=V+\Sigma_{sf\sigma}(E)\ , \tag{4.27}$$

then we get the final result (3.12) from (4.11) by some matrix inversions. More concretely, first we determine the averaged atomic T matrix $\langle t_\sigma\rangle$ by use of $\gamma_{i\sigma}$ and $\eta_{s,f\sigma}^{(i)}$ from Table I, $B_{s\sigma}$ from (4.5), and $B_{f\sigma}(E)$ from (4.7) in Eqs. (4.18)—(4.20). Second, $R_{ii\sigma}(E)$ follows from (4.2) and (4.9),

$$R_{ii\sigma}(E)=\frac{1}{N}\sum_{\mathbf{k}}R_{\mathbf{k}\sigma}(E)\ , \tag{4.28}$$

where $R_{\mathbf{k}\sigma}(E)$ has formally the same structure as $G_{\mathbf{k}\sigma}(E)$ in (3.12), we have only to replace $M_{\mathbf{k}\sigma}^{(s)}$ by $B_{s\sigma}$, $M_{\mathbf{k}\sigma}^{(f)}$ by $B_{f\sigma}$, and $\tilde{V}_\sigma$ by V. With $\langle t_\sigma\rangle$ and $R_{ii\sigma}$ the quantity $\Sigma_\sigma(E)$, in (4.24) is completely determined. Inserting (4.25)—(4.27) into (3.12) then provides us with a formal solution in terms of n_f,n_c,m_f,m_c, which is iterated to get the required self-consistent solution.

V. DISCUSSION OF THE RESULTS

The main problem that we want to discuss concerns the stability of the local $4f$ moment in situations, where the

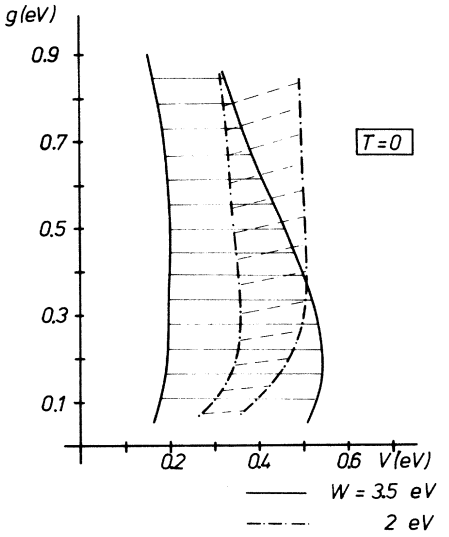

FIG. 3. Phase diagram as in Fig. 2, but now in terms of s-f hybridization V and s-f exchange g for two different Bloch bandwidths W (——, $W=3.5$ eV; —·—·—·, $W=2$ eV). Other parameters as in Fig. 1.

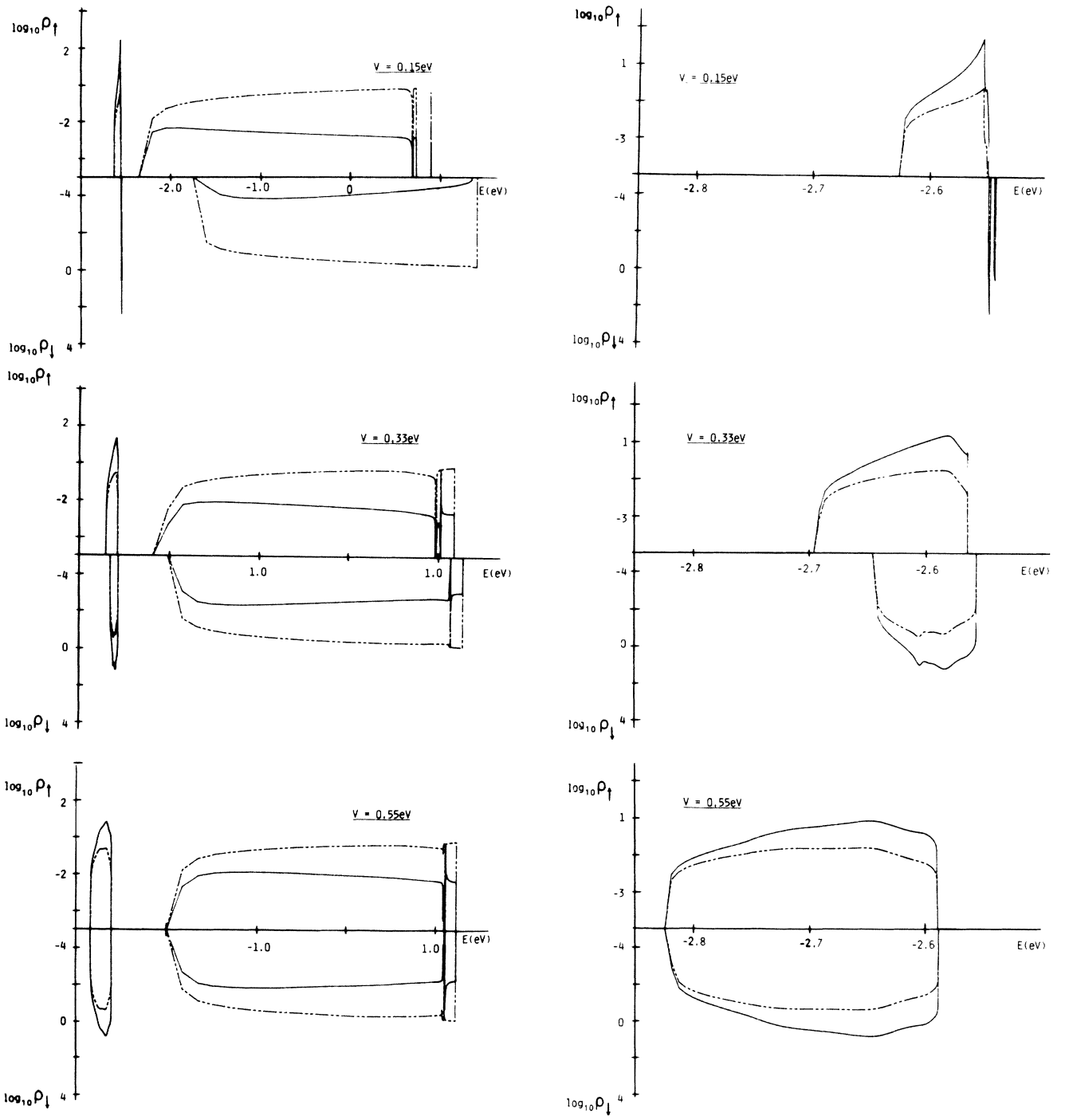

FIG. 4. Logarithms of the quasiparticle densities of states $\log_{10}\rho_{\uparrow\downarrow}^{(s,f)}$ as functions of energy E for three different values of the hybridization V and $W=3$ eV. Other parameters as in Fig. 1. Solid lines for $\rho_{\sigma}^{(f)}$, broken lines for $\rho_{\sigma}^{(s)}$. The low-energy peak of the left column is plotted in the right column on a larger scale.

system is driven by pressure or temperature variations or by alloying with proper impurities into an intermediate-valence phase. For this purpose we have investigated the influence of relevant physical quantities on the average f moment at $T=0$. As already mentioned in the Introduction, model parameters, which are *not* believed to have a direct relation to the phenomenon, are chosen appropriate to EuO. Relevant model parameters with respect to the stability of the local f moment are above all the s-f hybridization V and the Bloch bandwidth W, which simulates the pressure dependence, and also, of course, the exchange constants g and J_0.

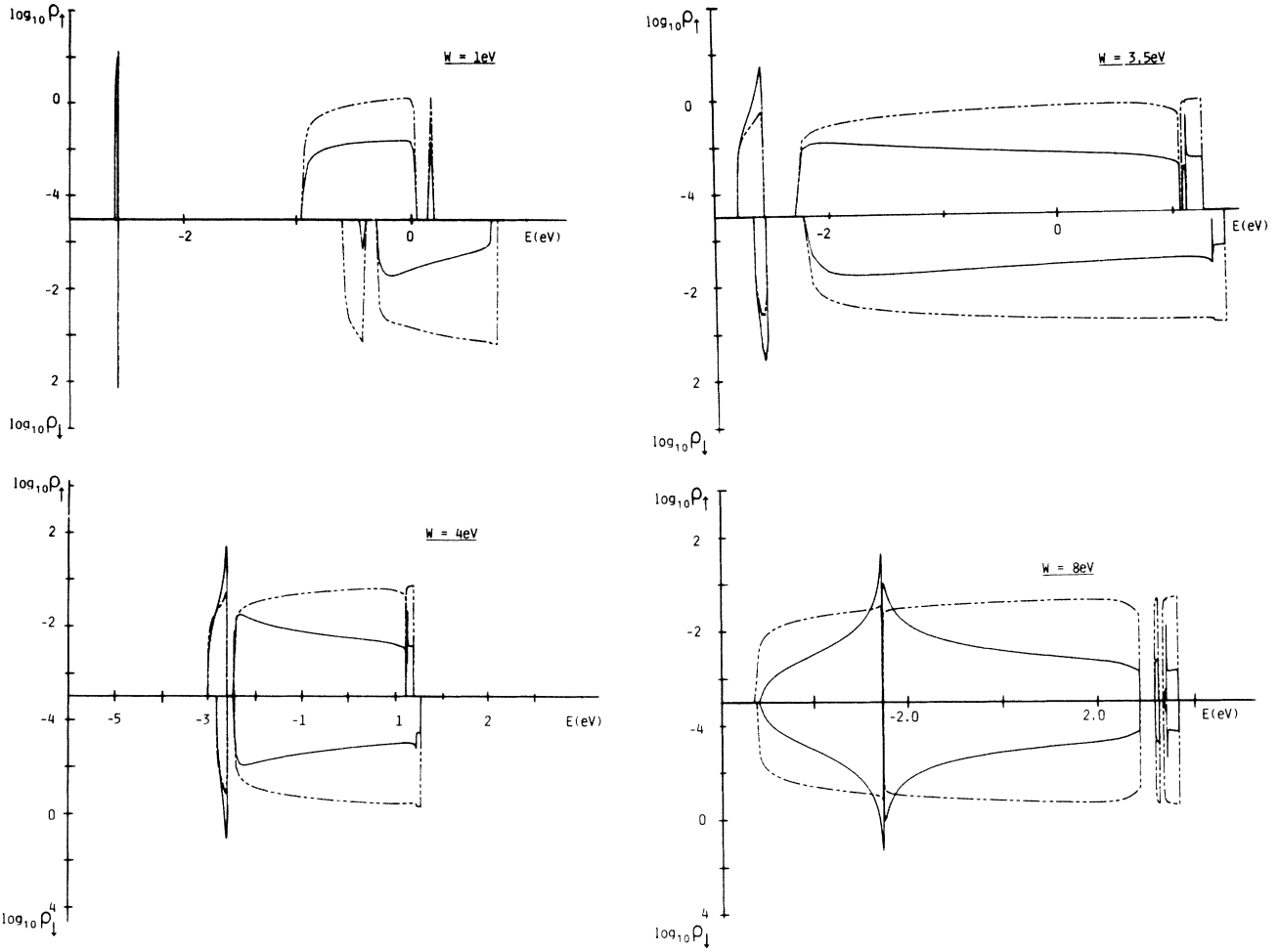

FIG. 5. Logarithms of the quasiparticle densities of states $\log_{10}\rho_{\uparrow\downarrow}^{(s,f)}$ as functions of energy for four different Bloch bandwidths W and $V=0.3$ eV. Other parameters as in Fig. 1. Solid lines for $\rho_\sigma^{(f)}$, broken lines for $\rho_\sigma^{(s)}$.

A. Phase diagrams ($T=0$)

Figure 1 shows the dependencies of the local moment on the s-f hybridization V and Bloch bandwidth W. As motivated in the Introduction we have fixed the distance between f level and the center of gravity of the Bloch band at the constant value of 2.54 eV ($T_0=0$, $E_f=-2.54$ eV). An external pressure p alters the Bloch bandwidth W, so that the W dependence is implicitly a p dependence. For the model density of states of Eq. (2.13) the gap between $4f$ level and lower conduction-band edge would be closed exactly at $W_c=3.82$ eV if there were no interactions. This value is indicated as a dotted line in Fig. 1. The hybridization and more importantly the s-f interaction,[6,12] give rise, however, to certain edge shifts, so that the gap actually closes already at a smaller W.

We have found three (W,V) regions for the local moment m_f. One region belongs to the saturated moment $m_f=n_f$, another to a reduced moment $0<m_f<n_f$, and a third to a completely quenched moment $m_f=0$. The general trend is that an increasing s-f hybridization V as well as a decreasing gap, i.e., increasing W, tend to destabilize the local moment up to a total quenching. This is not surprising, since both parameter changes intensify the electronic fluctuations between f level and conduction band. More surprising may be the relatively large (W,V) region, where the f moment remains unaffected by the electronic fluctuations (below the solid line in Fig. 1). Particularly for small V we observe a stable $T=0$ moment far into the intermediate-valence phase, so that electron transitions into the conduction band result only in a dilution of the localized moment system. An additional moment quenching ($m_f<n_f$) happens for (W,V) values above the solid phase line in Fig. 1. On the right-hand side of the dashed-dotted phase boundary a nonzero f moment is no longer possible. There is an interesting bulge of the phase line just in the transition region between normal and intermediate-valence phases. This is a consequence of the dynamic interplay between the alteration in the s-f exchange, caused by the electron tunneling into the conduction band, and the sensitive reaction of the quasiparticle density of states as explained in the Introduction. To illustrate this we have plotted in the insert of Fig. 1 the moment m_f as a function of the hybridization V, and that for three typical bandwidths, corresponding to the normal valence phase ($W=2$ eV), to the intermediate-valence phase ($W=8$ eV), and to the transition region ($W=3.5$ eV). The just-mentioned dynamic interplay is

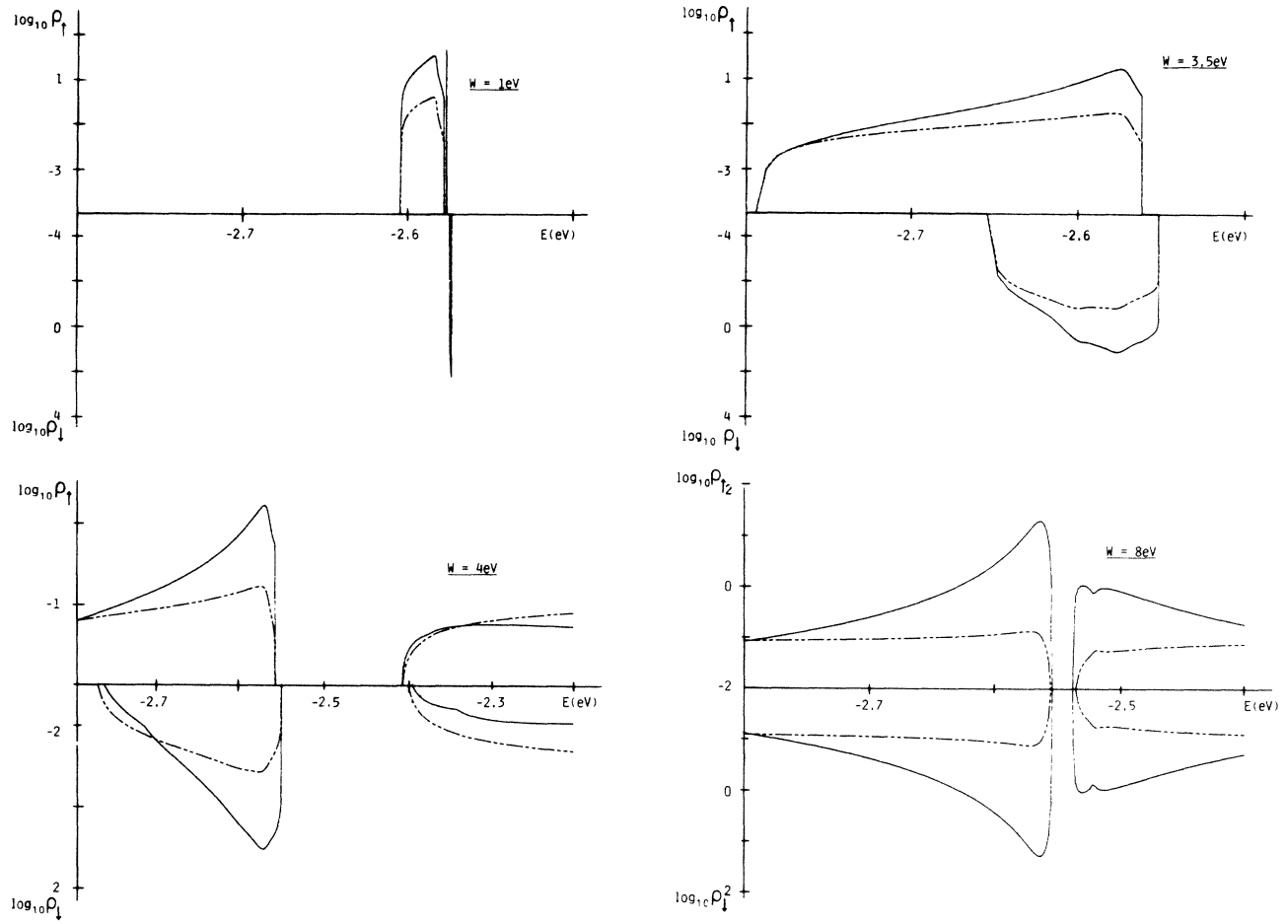

FIG. 6. Same as in Fig. 5, but now the original f peak (upper row) and the immediate surrounding of the hybridization gap (lower row) on a larger scale.

especially much in evidence in the transition region, where it gives rise to very-long-range tails in the m_f curves. It is an interesting detail that for small enough W ($W \lesssim 2$ eV) the local f moment cannot be totally quenched, no matter how large V is.

The phase diagram in Fig. 1 is drawn for constant s-f and f-f exchange couplings g and J_0, respectively ($g=0.2$ eV, $J_0=0.005$ eV). The influence of the direct exchange J_0 can be read off from Fig. 2. Increasing J_0 stabilizes the local moment, but ferromagnetism is possible even in the limit $J_0 \to 0$, as a consequence of a nonzero s-f exchange. The dependence on the s-f coupling g, shown in Fig. 3, reveals some interesting aspects, because g has obviously two consequences. Firstly it stabilizes, similar to J_0, the f moment. But on the other hand, the s-f exchange interaction takes care for a red shift of the lower conduction-band edge of about $\frac{1}{2}gSm_f/n_f$, leading therewith to an additional gap reduction. Smaller gap, however, means more electronic transitions, which destabilize the f moment. These two competitive consequences of the s-f exchange are best observable for Bloch bandwidths W, which are close to $W_c=3.82$ eV, the value at which the gap closes in the noninteracting system. For the example $W=3.5$ eV, plotted in Fig. 3, the magnetic region is maximal at $g=0.2$ eV, but decreases strongly with a further increasing of the s-f coupling. For $g>0.2$ eV the system undergoes an exchange-induced transition into the intermediate-valence phase.

B. Quasiparticle densities of states ($T=0$)

The just-discussed phase diagrams are in the last analysis direct consequences of the corresponding behavior of the quasiparticle densities of states $\rho_\sigma^{(s)}(E)$ and $\rho_\sigma^{(f)}(E)$, defined in Eq. (3.14). Figures 4–7 exhibit some typical examples. Figure 4 demonstrates the influence of the hybridization V on the densities of states. The left column shows $\rho_\sigma^{(s)}(E)$ (broken lines) together with $\rho_\sigma^{(f)}$ (solid lines) for a Bloch bandwidth $W=3$ eV and for three different hybridization matrix elements V, which belong to the regions of a saturated f moment $m_f=n_f$ ($V=0.15$ eV), of a reduced moment $0<m_f<n_f$ ($V=0.33$ eV), and of a quenched moment $m_f=0$ ($V=0.55$ eV). The relatively sharp peak at lower energies corresponds to the original f level E_f, being more and more smeared out with increasing V. The right column in Fig. 4 shows this peak on a larger scale. The Fermi edge

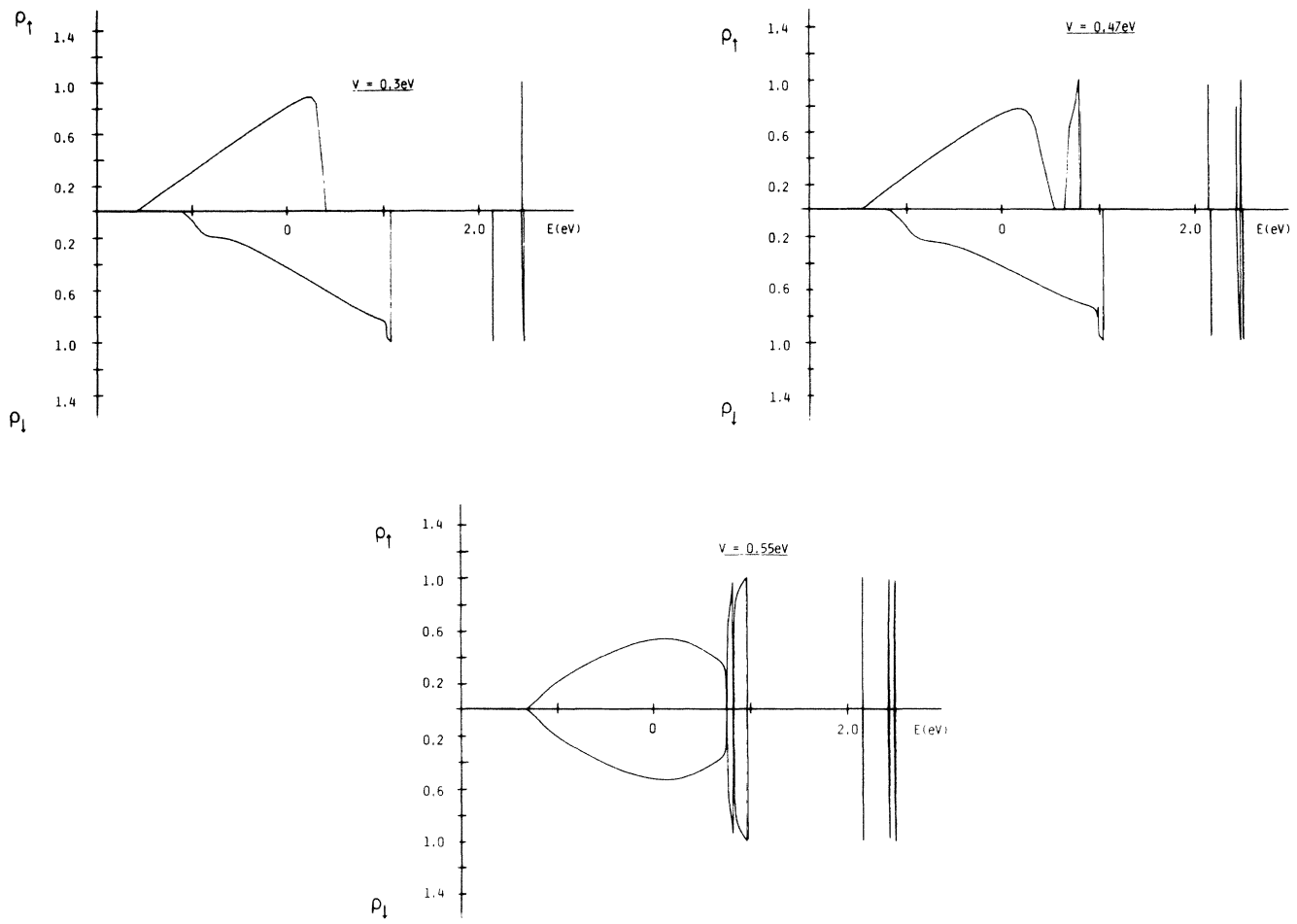

FIG. 7. s-quasiparticle density $\rho_\sigma^{(s)}$ of states as function of energy on a *linear* scale for three different values of the hybridization V and $W=2$ eV. Other parameters as in Fig. 1. The low-energy region around the original f level is not plotted.

is always at the upper edge of the spin-up peak. The relatively broad part of the spectrum, shown in the left column, refers to the original conduction band. Because of the hybridization H_v both densities of states $\rho_\sigma^{(s)}$ and $\rho_\sigma^{(f)}$ occupy exactly the same energy region, but usually being of different orders of magnitude. For the large hybridization $V=0.55$ eV spin-up and spin-down spectra coincide, so that there is no resulting f moment. With decreasing V the low-energy peak becomes sharper, and the spin-up and spin-down parts are shifted against another giving rise to a nonzero moment m_f. At $V=0.15$ eV the total spin-down spectrum lies above the Fermi edge, the moment m_f is saturated.

In that part of the spectrum, which belongs to the original conduction band, we observe a red shift of the lower edge with decreasing V, just as the temperature does in a normal ferromagnetic semiconductor. The original f peak shifts in the opposite direction, so that the gap is substantially reduced with decreasing V. For normal valent, ferromagnetic $4f$ systems such an edge shift is well known as a temperature effect. Cooling a ferromagnetic semiconductor like EuO from temperatures $T>T_c$ down to $T=0$ leads to a red shift of the conduction-band edge, which has just the same order of magnitude. The results of Fig. 4 are, however, found for $T=0$. Here the hybridization undertakes the role of the temperature. Decreasing V forces the system from a nonmagnetic into a magnetically saturated state.

The structure in the upper part of the spectrum is mainly due to the s-f interaction, which splits the original Bloch band in several quasiparticle subbands, as is already known from the normal s-f model.[12] Since the Fermi edge lies in the lower part of the spectrum, this structure does not directly influence the phase diagrams of Figs. 1–3.

Figure 5 shows the W dependence, and therewith the pressure dependence, of the quasiparticle densities of states for a hybridization $V=0.3$ eV. For $W=1$ eV the $4f$ system is still in its normal valence phase. The larger scale in Fig. 6 makes clear that the f moment is saturated ($m_f=n_f$), because the Fermi edge is again at the upper edge of the open-up peak. For $W=3.5$ eV the system is just in the transition region between normal and intermediate valence. The original f level is already smeared out to a narrow band, and the f moment is reduced (see Fig. 6). For $W=4$ eV the $4f$ system is now in its

intermediate-valence phase, but with a nonzero magnetic f moment. The latter becomes smaller with increasing W; at $W=0.8$ eV the moment is totally quenched. We observe an ever existing hybridization gap, which is the smaller the deeper the original f level has been shifted into the conduction band. The immediate surrounding of the hybridization gap has always dominant f character, particularly just below the gap.

To simplify the comparison of the results, presented here for the "hybridized" s-f model (2.1), with the previously published results for the "normal" s-f model,[12] we have plotted in Fig. 7 as an example the s density of states $\rho_\sigma^{(s)}(E)$ as function of energy on a *linear* scale. The similarity is obvious, but here appear some additional satellite peaks originating from the hybridization.

The fact that as a consequence of V $4f$ electrons can tunnel into the conduction band leads to nonmagnetic f levels and therewith to additional quasiparticle subbands. The high-energy peaks close to $\epsilon_6=U_c$ and $\epsilon_3=U_c+\frac{1}{2}gS$, respectively, have been omitted in Figs. 4–6, because they are not decisive for the phase diagrams.

VI. SUMMARY

We have used a "hybridized" s-f model in order to investigate the possibility of a coexistence of ferromagnetism and intermediate valence in systems which fluctuate between a magnetic and a nonmagnetic $4f$ configuration. The model should be realistic for systems which have a ferromagnetic ground state in the normal valence phase and, furthermore, a *positive* exchange coupling between localized $4f$ electrons and itinerant conduction electrons.

We have constructed three phase diagrams for the local magnetic f moment m_f at $T=0$. Phase boundaries separate regions of saturated ($m_f=n_f$), reduced ($0<m_f<n_f$), and quenched ($m_f=0$) moment. The general trend is that increasing hybridization V leads to a destabilization of the f moment up to a complete quenching. The same follows from a pressure-induced broadening of the conduction band, i.e., a gap reduction. There exist, however, parameter regions in which a coexistence of ferromagnetism and intermediate valence is possible. A direct exchange J_0, if present, stabilizes the magnetic moment. The influence is, however, not too dramatic. Ferromagnetism may appear even in the limit $J_0\to 0$, if only the s-f exchange g is unequal to zero. Increasing g stabilizes the moment, but also leads, on the other hand, to a gap reduction, which must be interpreted of course as a destabilizing effect.

The $T=0$—quasiparticle densities of states show a complicated structure as a consequence of the hybridization and the s-f interaction. In intermediate-valence phases an ever existing hybridization gap is observed.

ACKNOWLEDGMENTS

We are very grateful to A. Wunderlich for substantial support in many respects. One of us (A.R.) thanks Professor O. Krisement for hospitality.

*Permanent address: Department of Physics, Kakatiya University, Warangal-506009, India.

[1]See the review: J. M. Lawrence, P. S. Riseborough, and R. D. Parks, Rep. Prog. Phys. **44**, 1 (1981).
[2]C. M. Varma, Solid State Commun. **30**, 537 (1979).
[3]A. Jayaraman, A. K. Singh, A. Chatterjee, and S. Usha Devi, Phys. Rev. B **9**, 2513 (1974).
[4]W. Nolting, Z. Phys. B **49**, 87 (1982).
[5]H. G. Zimmer, K. Takemura, K. Fischer, and K. Syassen, Phys. Rev. B **29**, 2350 (1984).
[6]See the review by W. Nolting, Phys. Status Solidi B **96**, 11 (1979).
[7]D. Gignoux and J. Voiron, Phys. Lett. **108A**, 473 (1985).
[8]M. M. Abd-Elmeguid, C. Sauer, U. Köhler, W. Zinn, J. Röhler, and K. Keulerz, J. Magn. Magn. Mater. **47/48**, 417 (1985); Z. Phys. B **60**, 239 (1985).
[9]S. K. Malik, A. M. Umarji, G. K. Shenoy, P. A. Montano, and M. E. Reeves, Phys. Rev. B **31**, 4728 (1985); Solid State Commun. **54**, 761 (1985).
[10]M. Matlak and W. Nolting, Z. Phys. B **55**, 103 (1984).
[11]M. Matlak, W. Nolting, and A. M. Oleś, J. Magn. Magn. Mater. **47/48**, 577 (1985).
[12]W. Nolting, Phys. Rev. B **32**, 402 (1985).
[13]W. Nolting, U. Dubil, and M. Matlak, J. Phys. C **18**, 3687 (1985).
[14]W. Nolting, and A. M. Olés, J. Phys. C **13**, 823 (1980).
[15]F. Yonezawa and L. Morigaki, Prog. Theor. Phys. Suppl. **53**, 1 (1973).
[16]K. Ueda, Solid State Commun. **41**, 375 (1982).
[17]E. Baech and G. Czycholl, Solid State Commun. **43**, 89 (1982).
[18]M. Plischke, Phys. Rev. Lett. **28**, 361 (1972).
[19]D. K. Ghosh, Solid State Commun. **18**, 1377 (1976).
[20]W. Nolting and M. Matlak, Phys. Status Solidi B **123**, 155 (1984).
[21]L. Schwartz, F. Broners, A. V. Vedyayev, and H. Ehrenreich, Phys. Rev. B **4**, 3383 (1971).